



## **Transmission electron microscopy study of epitaxial La<sub>0.8</sub>MnO<sub>3</sub> thin films on SrTiO<sub>3</sub>**

Jun Chen, Jing Zhu

### **► To cite this version:**

Jun Chen, Jing Zhu. Transmission electron microscopy study of epitaxial La<sub>0.8</sub>MnO<sub>3</sub> thin films on SrTiO<sub>3</sub>. Philosophical Magazine, 2006, 86 (27), pp.4341-4350. <10.1080/14786430600696363>. <hal-00513695>

**HAL Id: hal-00513695**

**<https://hal.science/hal-00513695v1>**

Submitted on 1 Sep 2010

**HAL** is a multi-disciplinary open access archive for the deposit and dissemination of scientific research documents, whether they are published or not. The documents may come from teaching and research institutions in France or abroad, or from public or private research centers.

L'archive ouverte pluridisciplinaire **HAL**, est destinée au dépôt et à la diffusion de documents scientifiques de niveau recherche, publiés ou non, émanant des établissements d'enseignement et de recherche français ou étrangers, des laboratoires publics ou privés.



HAL Authorization



# **Transmission electron microscopy study of epitaxial La<sub>0.8</sub>MnO<sub>3</sub> thin films on SrTiO<sub>3</sub>**

Journal:	<i>Philosophical Magazine &amp; Philosophical Magazine Letters</i>
Manuscript ID:	TPHM-05-Nov-0501.R1
Journal Selection:	Philosophical Magazine
Date Submitted by the Author:	09-Mar-2006
Complete List of Authors:	Chen, Jun; Tsinghua University, Materials Science and Engineering Zhu, Jing; Tsinghua University, Materials Science and Engineering
Keywords:	microstructure, transmission electron microscopy
Keywords (user supplied):	La <sub>0.8</sub> MnO <sub>3</sub>



**Transmission electron microscopy study of epitaxial  $\text{La}_{0.8}\text{MnO}_3$  thin films on  $\text{SrTiO}_3$**

J. CHEN and J. ZHU\*

Electron Microscope Laboratory, School of Material Science and Engineering,  
Tsinghua University, Beijing, 100084, China

\* Corresponding author:

Professor Jing Zhu

Electron Microscope Laboratory, School of Materials Science and Engineering, Tsinghua  
University, Beijing 100084, P.R. China

E-mail address: [jzhu@mail.tsinghua.edu.cn](mailto:jzhu@mail.tsinghua.edu.cn)

Telephone: 86-10-62794026

Fax: 86-10-62772507

Structure and microstructure of  $\text{La}_{0.8}\text{MnO}_3$  thin films on  $\text{SrTiO}_3$  substrates fabricated by pulsed laser deposition with substrate temperatures of 873K and 1073K, respectively, have been studied by transmission electron microscopy. In both films, a columnar growth morphology has been observed. The columnar grain size is found to increase with increasing substrate temperature. In the film deposited with the substrate temperature of 1073K, there is only one rhombohedral phase. However, two phases, a rhombohedral one and an orthorhombic one, have been observed in the film deposited at 873K.

**Keywords:**  $\text{La}_{0.8}\text{MnO}_3$ ; Transmission electron microscopy; Microstructure

## 1. Introduction

Recently there has been great interest in studying the magnetoresistive properties of the doped perovskite  $\text{La}_{1-x}\text{R}_x\text{MnO}_3$  ( $\text{R}=\text{Ba}, \text{Ca}, \text{Sr}, \text{and Pb}$ ) [1-4]. These external-doped manganese oxides are known to be conducting and ferromagnetic below Curie temperature and exhibit colossal magnetoresistance (CMR) effect. The basic manganite  $\text{LaMnO}_3$  is antiferromagnetic and insulating [5]. The substitution of lanthanum by divalent valency ions induces a mixed valency of  $\text{Mn}^{3+}$  and  $\text{Mn}^{4+}$ , which is responsible for the magnetic double exchange interaction and thus for the magnetoresistive properties [6].

Self-doped lanthanum manganites, represented by the general formula  $\text{La}_{1-x}\text{MnO}_3$ , are interesting because they exhibit similar properties as that of the external-doped manganites. In  $\text{La}_{1-x}\text{MnO}_3$ , the lanthanum deficiency produces a mixed  $\text{Mn}^{3+}/\text{Mn}^{4+}$  valency similar to that in divalent substituted compounds, which could lead to the CMR effect. A magnetoresistance of 85% under 6T was obtained in  $\text{La}_{0.7}\text{MnO}_3$  films on  $\text{LaAlO}_3$  prepared by pulsed laser deposition (PLD) with a substrate temperature of 993K [7]. Gupta *et al.* [8] reported a magnetoresistance of 55% under 4T in  $\text{La}_{0.75}\text{MnO}_3$  films grown by PLD on  $\text{SrTiO}_3$  at 973K.

In order to understand the interplay of structure, magnetism and electronic transport of the manganese oxides, it is of great importance to study their microstructures. [9-13] Transmission electron microscopy (TEM) is a powerful tool for characterization of microstructures in materials. In the past few years TEM has been widely applied in the studies of CMR materials, and particularly in thin films of external-doped lanthanum manganites [13-28]. Van Tendeloo *et al.* [15] reported that  $\text{La}_{0.7}\text{Sr}_{0.3}\text{MnO}_3$  films with a rhombohedral structure on  $\text{LaAlO}_3$  were elastically strained but the stress was partially relaxed when the film thickness was over 30-

35nm. In  $\text{La}_{1-x}\text{Ca}_x\text{MnO}_3$  films on  $\text{SrTiO}_3$ , a thin featureless and coherent layer with a thickness of about 50nm was found and subsequently a second thicker layer was grown featuring a columnar microstructure. This so-called featureless layer was also observed in  $\text{La}_{0.7}\text{Ca}_{0.3}\text{MnO}_3$  on  $\text{LaAlO}_3$ , and on top of this layer, oriented domains were found [21]. Comparing with the large amount of studies on the structures and microstructures of  $\text{La}_{1-x}\text{R}_x\text{MnO}_3$  films, there are fewer reports on those of  $\text{La}_{1-x}\text{MnO}_3$  films [29, 30].

In this work, lanthanum-deficient  $\text{La}_{0.8}\text{MnO}_3$  (LMO) thin films on  $\text{SrTiO}_3(001)$  (STO) were prepared by pulsed laser deposition with substrate temperatures of 873K and 1073K, respectively. Both films exhibit columnar growth morphologies and the columnar grain size is found to increase with increasing substrate temperature. In the film deposited with the substrate temperature of 1073K, there is only one rhombohedral phase, while in the film deposited with a substrate temperature of 873K, a coexistence of two phases, a rhombohedral one and an orthorhombic one, has been observed.

## 2. Experimental methods

LMO films were deposited from a ceramic target of  $\text{La}_{0.8}\text{MnO}_3$  on  $\text{SrTiO}_3(001)$  substrate by PLD with substrate temperatures of 873K and 1073K, respectively. The deposition was performed with a KrF excimer laser (248nm, Lambda Physik). During deposition, a background oxygen pressure of 40Pa was maintained. The laser energy fluence and pulse repetition frequency were  $1.5\text{J}/\text{cm}^2$  and 5Hz, respectively. After deposition, the films were cooled down to room temperature under  $10^{-5}\text{Pa}$  of oxygen at 20K/min. The thicknesses of the films were calculated according to the deposition time and verified by TEM.

Cross-sectional specimens were prepared by mechanical thinning down to ~30µm followed by ion milling to electron transparency. TEM observations were performed in a JEM-2010F field emission gun transmission electron microscope operated at 200kV with a point resolution of 0.23nm. Low magnification TEM images were used to investigate the morphology of the films. Electron diffraction patterns and High-resolution electron microscopy were used to investigate the structure and microstructure of the films. The film composition (La/Mn) was determined using Rutherford backscattering spectrometry (RBS) and X-ray energy dispersive spectroscopy (EDS). The RBS results showed that the ratio of La/Mn is 0.80 in the films, the same as the target's. Series of EDS were acquired from different regions in the films and the results indicated that the ratio of La/Mn is  $0.80 \pm 0.02$ .

3. Results and discussion

3.1. Low magnification TEM images

Figure 1 shows the low magnification TEM images taken from the cross-sectional samples of the two films. In both films, a thin featureless layer with a thickness of ~50nm was formed on the substrate and subsequently a second layer was grown featuring a columnar structure. The white contrast regions are columnar grain boundaries which are almost perpendicular to surface of the substrate. The columnar grain size is found to increase with increasing substrate temperature. This columnar growth morphology has also been observed in the external-doped films of  $\text{La}_{0.7}\text{Ca}_{0.3}\text{MnO}_3$  prepared by PLD on  $\text{SrTiO}_3$  [19] and  $\text{La}_{0.8}\text{Sr}_{0.2}\text{MnO}_3$  prepared by PLD on  $\text{LaAlO}_3$  [20].

[Insert figure 1 about here]

### 3.2. Electron diffraction patterns and High-resolution electron microscopy

In the LMO film deposited with a substrate temperature of 873K, two types of electron diffraction patterns (EDPs) are frequently observed, as shown in Figure 2 from the cross-section sample of the film. Figure 2 (a), (b) and (c) are a series of EDPs taken from a region at the film surface along different directions by tilting the specimen. It shows that LMO film surface belongs to rhombohedral structure with a space group of  $R\bar{3}c$  and hexagonal lattice parameters,  $a_H \approx \sqrt{2}a_p$ ,  $c_H \approx 2\sqrt{3}a_p$  ( $a_p$  is the lattice parameter of the undistorted perovskite unit cell), which has been reported in  $\text{La}_{1-x}\text{MnO}_{3+\delta}$  bulk before [31-34].

[Insert figure 2 about here]

Figure 2 (d), (e) and (f) are a series of EDPs taken from a region near the interface between the film and the substrate along different directions by tilting the specimen, showing orthorhombic structure of  $Pnma$  space group, which also has been reported in  $\text{La}_{1-x}\text{MnO}_{3+\delta}$  bulk before [31-34]. The lattice parameters of  $Pnma$  orthorhombic structure are  $a_o \approx \sqrt{2}a_p$ ,  $b_o \approx 2a_p$  (The footnotes o and p refer to the orthorhombic unit cell and ideal perovskite unit cell, respectively). Figure 2(d) shows superposition of EDPs along [010] and [101] directions. Figure 2(e) shows superposition of EDPs along [131], [313] and [201] directions. Figure 2(f) shows superposition of EDPs along [121], [212] and [301] directions. It indicates that there are three types of oriented domains near the film-substrate interface. According to the diffraction condition of  $Pnma$  space group ( $0kl : k+l=2n$ ,  $hk0 : h+k=2n$ ,  $h00 : h=2n$ ,  $0k0 : k=2n$ ,  $00l : l=2n$ ), some reflections in Figure 2 (d), (e) and (f) are forbidden, such as  $h00 : h=2n+1$ ,  $0k0 : k=2n+1$ ,  $00l : l=2n+1$ . However,



these forbidden reflections can be caused by double diffraction effects, e.g.,

$$g_{100} = g_{101}^- + g_{201}^-, g_{010} = g_{111}^- + g_{101}^-, g_{001} = g_{101}^- + g_{102}^-.$$

Figure 3(a) shows the High-resolution image of the LMO/STO interface for the film deposited with the substrate temperature of 873K. Figure 3 (b), (c) and (d) are Fourier transformation patterns corresponding to area 1, 2 and 3 in Figure 3(a), respectively. It can be seen that three types of orthorhombic oriented domains originate from the interface between the LMO film and STO substrate. The domain sizes range from several nanometers to tens of nanometers. The orientation relation between the oriented domains and STO substrate is specific and listed as follows:

Domain 1: LMO(010)//STO(001), LMO[101]//STO[100]

or LMO(010)//STO(001), LMO[10 $\bar{1}$ ]//STO[100]

Domain 2: LMO(101)//STO(001), LMO[010]//STO[100]

or LMO(10 $\bar{1}$ )//STO(001), LMO[010]//STO[100]

Domain 3: LMO(101)//STO(001), LMO[101]//STO[100]

or LMO(10 $\bar{1}$ )//STO(001), LMO[101]//STO[100]

There are six possible orientation relationships between the LMO film and substrate, however, due to the pseudocubic perovskite unit cell of LMO, only three types of oriented domains can be observed in the film.

[Insert figure 3 about here]

The dimensions of each domain are so small that conventional selected area diffraction, even using the smallest aperture in ordinary TEM, may only give composite EDPs. To obtain EDPs from a single domain, we used nanodiffraction technique with the spot size of several nanometers. Figure 4 are the nanodiffraction patterns taken from different areas in a single columnar grain. **Figure 4 (a) and (b)**

were taken from regions near the film/substrate interface and Figure 4(c) was taken from a region far away from the film/substrate interface. Figure 4(a) indicates a [010] oriented orthorhombic domain; Figure 4(b) indicates a  $[10\bar{1}]$  oriented orthorhombic domain; Figure 4(c) indicates  $[42\bar{1}]_H$  zone of rhombohedral structure. The NBD patterns show that different types of orthorhombic oriented domains exist in column grains and in regions far from the interface the film displays rhombohedral structure.

The existence of orthorhombic oriented domains both in the featureless layer and columnar grains shows that oriented domains are intermixed in three dimensions, which can be rationalized by their inherent pseudosymmetry. The domain boundaries seem diffuse and sometimes are high-index crystal planes.

[Insert figure 4 about here]

In the LMO film deposited with the substrate temperature of 1073K, the regions near the film/substrate interface and the regions far from the interface have the same type of EDP as shown in Figure 5(a), which indicates that the film belongs to rhombohedral structure of  $R\bar{3}c$  space group. Figure 5(b) shows the High-resolution image of the LMO/STO interface in the film deposited with the substrate temperature of 1073K. Figure 5(c) is Fourier transformation pattern of the LMO part in Figure 5(b), which indicates that the interface between the film and the substrate has rhombohedral structure with  $R\bar{3}c$  space group. Thus, the results of EDP and High-resolution image suggest that there is only rhombohedral phase in the LMO film deposited with the substrate temperature of 1073K.

[Insert figure 5 about here]

#### 4. Discussion

The columnar growth morphology is demonstrated to originate from mismatch between the film and the substrate by Zheng *et al.* [10], and the columnar structure is a method of relaxing the stress. In the  $\text{La}_{0.8}\text{MO}_3$  films on  $\text{SrTiO}_3$ , the distance between  $\{101\}_o$  lattice planes of  $\text{La}_{0.8}\text{MO}_3$  is 0.388nm [35], while the distance of the  $\text{SrTiO}_3\{010\}$  planes is 0.3905nm. So the film is under an in-plane tensile stress when it grows epitaxially on the  $\text{SrTiO}_3$  substrate. So that the columnar growth morphology is observed in both films prepared by PLD in the present work. During deposition, when the substrate temperature is higher, the mobility of atoms on the substrate is larger. So the columnar grain size is larger in the film deposited at 1073K than at 873K, which is consistent with the results reported by Wang *et al.* [11, 12].

Both  $R\bar{3}c$  rhombohedral structure and  $Pnma$  orthorhombic structure can be derived from the undistorted configuration of perovskite by tilting the  $\text{MnO}_6$  octahedra with different tilt systems of  $a^-a^-a^-$  and  $a^+b^-b^-$  [36, 37], respectively. In  $\text{La}_{0.8}\text{MO}_3$  film deposited with the substrate temperature of 873K, the stress in the region near the interface is larger than that far from the interface. This causes deformation of the  $\text{MnO}_6$  octahedra in the film near the interface and changes  $\text{La}_{0.8}\text{MO}_3$  from the rhombohedral into the orthorhombic phase. Besides strain induced transformation, there is also thermally induced transformation from orthorhombic to rhombohedral, which has been reported in  $\text{La}_{1-x}\text{MnO}_{3+\delta}$  bulk [31-34]. Shu *et al.* [34] reported that the crystal symmetry of orthorhombic  $\text{La}_{0.95}\text{MnO}_3$  bulk increases from orthorhombic to rhombohedral in temperature range of 373K-473K due to the depression of Jahn-Teller distortion. During the deposition of  $\text{La}_{0.8}\text{MO}_3$  film, the higher deposition temperature provides higher energy and atom

mobility, thus only rhombohedral phase can be observed in  $\text{La}_{0.8}\text{MO}_3$  film deposited with the substrate temperature of 1073K.

The formation of oriented domains of *Pnma* structure has been largely reported not only in  $\text{La}_{1-x}\text{R}_x\text{MnO}_3$  ( $\text{R} = \text{Ca}, \text{Sr}$  or vacancy) thin films [13-25], but also reported in  $\text{A}_{1-x}\text{R}_x\text{MnO}_3$  ( $\text{A} = \text{Pr}$  or  $\text{La}$ ;  $\text{B} = \text{Sr}$  or  $\text{Ca}$ ) bulk materials [26, 27]. Thus, it seems that the formation of oriented domains originates from the inherent pseudosymmetry of the structure itself rather than induced by the substrate. However, Aarts *et al.* [13] reported that the type of oriented domains is dependant on the film thickness. As the film thickness increased from 5nm to more than 30nm, the microstructure of films turned from pure [001] oriented from mixed domains of [001] and [110] orientation. Similar phenomenon has also been reported by Rao *et al.* [9] and Yang *et al.* [16]. Compared with previous reports, the coexistence of three types of oriented domains of orthorhombic structure in  $\text{La}_{0.8}\text{MO}_3$  film with the substrate deposition temperature of 873K is rationalized due to the inherent pseudosymmetry of the structure and the 400nm film thickness.

## 5. Conclusions

TEM has been used to characterize thin films of  $\text{La}_{0.8}\text{MO}_3$  prepared by PLD on  $\text{SrTiO}_3$  substrates. Low magnification TEM images show that both films deposited with substrate temperature of 873K and 1073K follow the columnar growth morphology.

In the films deposited with a substrate temperature of 1073K, only rhombohedral phase has been observed. However, in the films with a substrate temperature of 873K, besides rhombohedral phase, another orthorhombic phase in the form of oriented domains have been observed. This can be explained by

1  
2  
3  
4  
5  
6  
7  
8  
9  
10  
11  
12  
13  
14  
15  
16  
17  
18  
19  
20  
21  
22  
23  
24  
25  
26  
27  
28  
29  
30  
31  
32  
33  
34  
35  
36  
37  
38  
39  
40  
41  
42  
43  
44  
45  
46  
47  
48  
49  
50  
51  
52  
53  
54  
55  
56  
57  
58  
59  
60

considering both strain induced transformation and thermally induced transformation.

**Acknowledgements**

This work is financial supported by the National 973 Project of China, Chinese National Nature Science Foundation and National Center for Nanoscience and Technology of China.

## References

- [1] R.M. Kusters, J. Singleton, D.A. Keon, *et al.*, Physica B **155** 362 (1989).
- [2] R. Von Helmolt, J. Wecker, B. Holzapfel, *et al.*, Phys. Rev. Lett. **71** 2331 (1993).
- [3] K. Chabara, T. Ohno, M. Kasai, *et al.* Appl. Phys. Lett. **63** 1190 (1993).
- [4] S. Jin, T.H. Tiefel, M. McCormack, *et al.*, Science **264** 413 (1994).
- [5] S.V. Pietambaram, D. Kumar, R.K. Singh, *et al.*, J. Appl. Phys. **86** 3317 (1999).
- [6] C. Zener, Phys. Rev. **82** 403 (1951).
- [7] S. Manoharan, N.Y. Vasanthacharya, M.S. Hedge, *et al.*, J. Appl. Phys. **76** 3923 (1994).
- [8] A. Gupta, T.R. McGuire, P.R. Duncombe, *et al.*, Appl. Phys. Lett. **67** 3494 (1995).
- [9] R.A. Rao, D. Lavric, T.K. Nath, *et al.*, Appl. Phys. Lett. **73** 3294 (1998).
- [10] X. Zheng, C.C. Wang and J. Zhu, J. Magn. magn. Mater. **267** 168 (2003).
- [11] C.C. Wang, H. Wang, X. Zheng, *et al.*, Appl. Phys. A **81** 1423 (2005).
- [12] C.C. Wang, H. Wang and J. Zhu, J. Appl. Phys. **97** 086104-1 (2005).
- [13] J. Aarts, S. Freisem, R. Hendrikx, *et al.*, Appl. Phys. Lett. **72** 2975 (1998).
- [14] X.L. Ma, Y.L. Zhu, X.M. Meng, *et al.*, Phil. Mag. A **82** 1331 (2002).
- [15] G. Van Tendeloo, O.I. Lebedev and S. Amelinckx, J. Magn. Magn. Mater. **211** 73 (2000).
- [16] Z.Q. Yang, R. Hendrikx, J. Aarts, *et al.*, Phys. Rev. B **70** 174111 (2004).
- [17] M. Zhang, X.L. Ma and D.X. Li, Phil. Mag. **85** 1625 (2005).
- [18] Y.L. Zhu, X.L. Ma, M. Zhang, *et al.*, Mater. Lett. **58** 1485 (2004).
- [19] O.I. Lebedev, G. Van Tendeloo, S. Amelinckx, *et al.*, Phys. Rev. B **58** 8065 (1998).
- [20] J.C. Jiang, E.I. Meletis and K.I. Gnanasekar, J. Mater. Res. **18** 2556 (2003).

- [21] C.J. Lu, Z.L. Wang, C. Kwon, *et al.*, J. Appl. Phys. **88** 4032 (2000).
- [22] P.G. Radaelli, G. Iannone, M. Marezio, *et al.*, Phys. Rev. B **56** 8265 (1997).
- [23] H.W. Zandbergen, S. Freisem, T. Nojima, *et al.*, Phys. Rev. B **60** 10259 (1999).
- [24] H.W. Zandbergen, J. Jansen, S. Freisem, *et al.*, Phil. Mag. A **80** 337 (2000).
- [25] K. Frohlich, I. Vavra, F. Gomory, *et al.*, J. Magn. Magn. Mater. **211** 67 (2000).
- [26] M.Hervieu, G. Van Tendeloo, V. Caignaert, *et al.*, Phys. Rev. B **53** 14274 (1996).
- [27] M.V. Lobanov, A.M. Balagurov, V.J. Pomjakushin, *et al.*, Phys. Rev. B **61** 8941 (2000).
- [28] Q.Zhan, R. Yu, L.L. He, *et al.*, Phys. Rev. Lett. **88** 196104-1 (2002).
- [29] H. Vincent, M. Audier, S. Pignard, *et al.*, J. Solid State Chem. **164** 177 (2002).
- [30] A. Boask, C. Dubourdieu, M. Audier, *et al.*, Appl. Phys. A **79** 1979 (2004).
- [31] P. Norby, I.G. Krogh Andersen, *et al.*, J. Solid State Chem. **119** 191 (1995).
- [32] J.A.M. Van Roosmalen, P. Van Vlaanderen, E.H. P. Cordfunke, *et al.*, J. Solid State chem. **114** 516 (1995).
- [33] Q. Huang, A. Santoro, R.W. Erwin, *et al.*, Phys. Rev. B **55** 14987 (1997).
- [34] Q. Shu, J. Zhang and J. Liu, J. Alloys Compds. **390** 240 (2005).
- [35] S. Pignard, H. Vincent, J.P. Senateur, *et al.*, J. Appl. Phys. **82** 4445 (1997).
- [36] A.M. Glazer, Acta. Crystallogr. B **28** 3384 (1972).
- [37] A.M. Glazer, Acta Crystallogr. A **31** 756 (1975).

### Captions of figures:

Figure 1. Low-magnification cross-section TEM images of LMO films deposited with the substrate temperature of (a) 873K and (b) 1073K, respectively, along [010] zone of STO substrates.

Figure 2. Selected area electron diffraction (SAED) patterns of LMO film deposited with the substrate temperature of 873K. (a), (b) and (c) SAED patterns taken from a region at the film surface along  $[42\bar{1}]_H$ ,  $[20\bar{1}]_H$  and  $[51\bar{2}]_H$  by tilting the specimen, showing rhombohedral structure, indexed with hexagonal unit cell. (d), (e) and (f) SAED patterns taken from a region near the interface between the film and the substrate by tilting the specimen, showing orthorhombic structure in the form of microdomains with three different orientations, indexed with orthorhombic unit cell.

Figure 3. (a) High-resolution image of the LMO/STO interface for the film deposited with the substrate temperature of 873K. (b), (c) and (d) Fourier transformation patterns corresponding to area 1, 2 and 3 in (a), respectively. It can be seen that three types of orthorhombic oriented domains originate from the interface between the LMO film and STO substrate.

Figure 4. Electron nanodiffraction patterns (NBD) taken from different parts of a columnar grain along the growth direction of LMO film deposited with the substrate temperature of 873K. (a) NBD of  $[010]_O$  oriented orthorhombic domain, (b) NBD of  $[10\bar{1}]_O$  oriented orthorhombic domain and (c) NBD indexed as  $[42\bar{1}]_H$  zone of



1  
2  
3  
4  
5  
6  
7  
8  
9  
10  
11  
12  
13  
14  
15  
16  
17  
18  
19  
20  
21  
22  
23  
24  
25  
26  
27  
28  
29  
30  
31  
32  
33  
34  
35  
36  
37  
38  
39  
40  
41  
42  
43  
44  
45  
46  
47  
48  
49  
50  
51  
52  
53  
54  
55  
56  
57  
58  
59  
60

rhombohedral structure. It indicates that there are different types of oriented domains in columnar grains.

Figure 5. (a) SAED pattern of LMO film deposited with the substrate temperature of 1073K. (b) High-resolution image of the LMO/STO interface in the film deposited with the substrate temperature of 1073K. (c) Fourier transformation pattern of the LMO part in Figure 5(b)

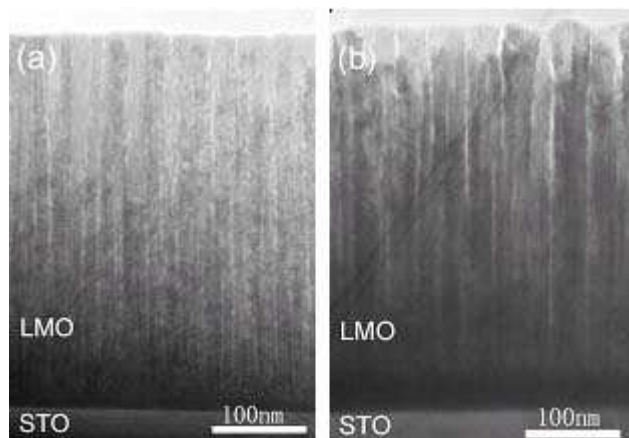


Figure 1  
110x77mm (72 x 72 DPI)

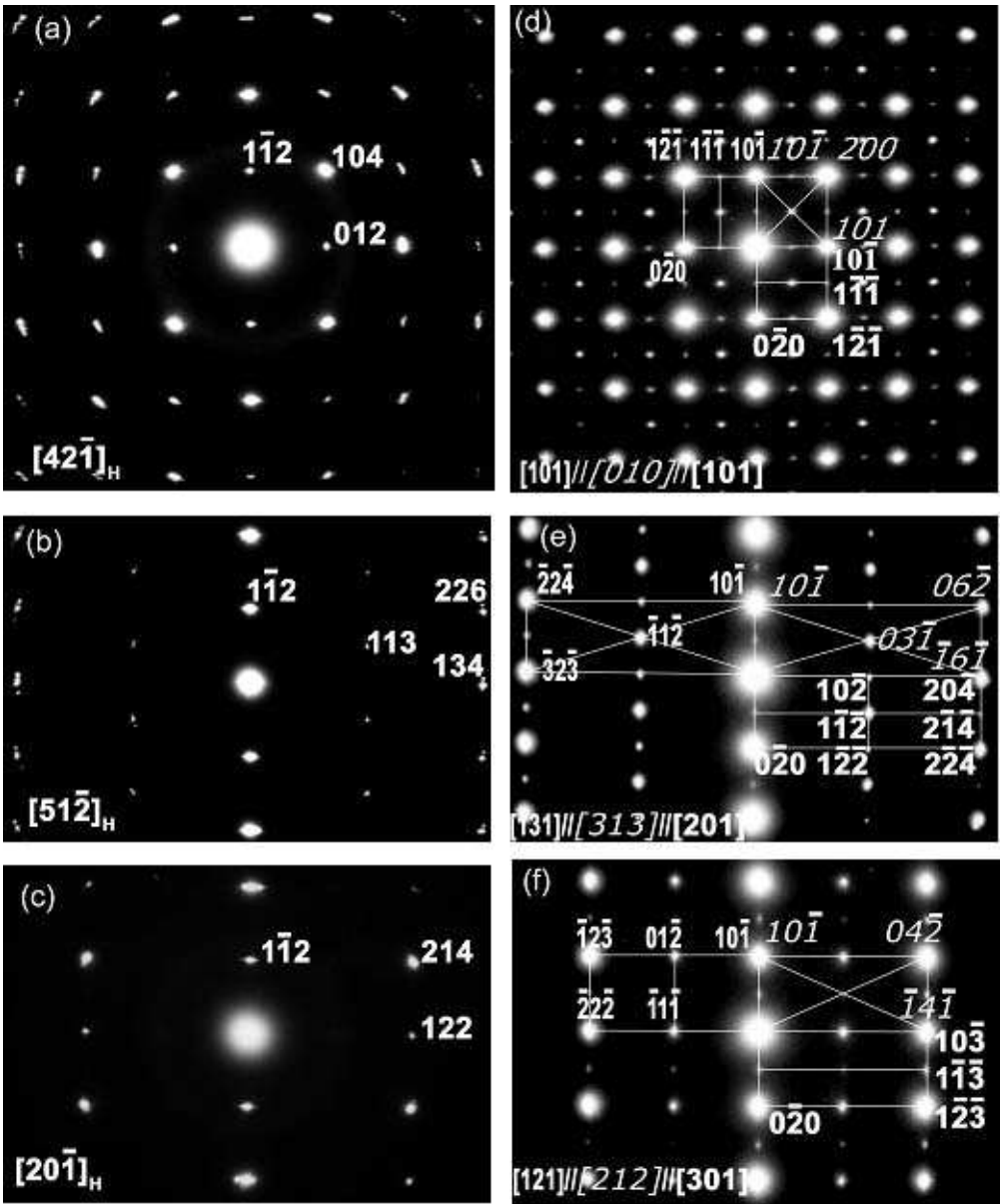


Figure 2  
183x220mm (72 x 72 DPI)

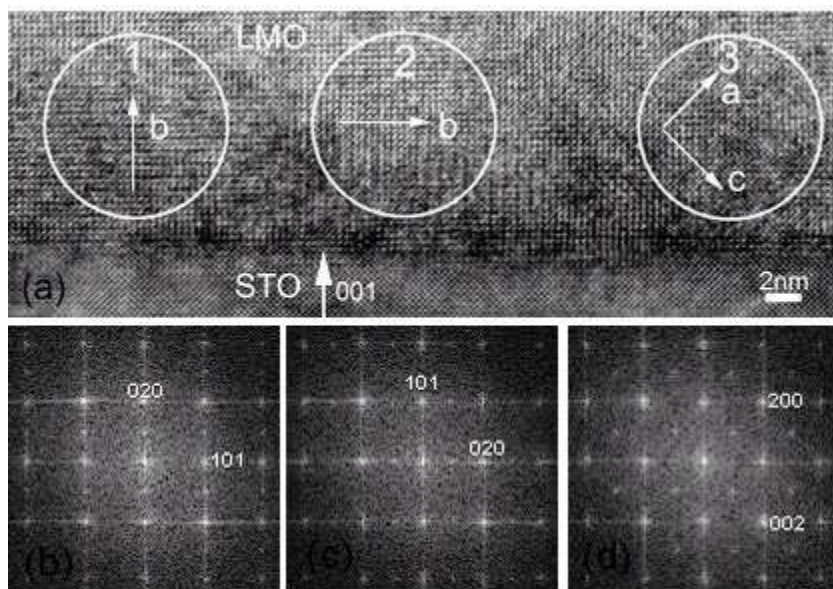


Figure 3  
146x105mm (72 x 72 DPI)

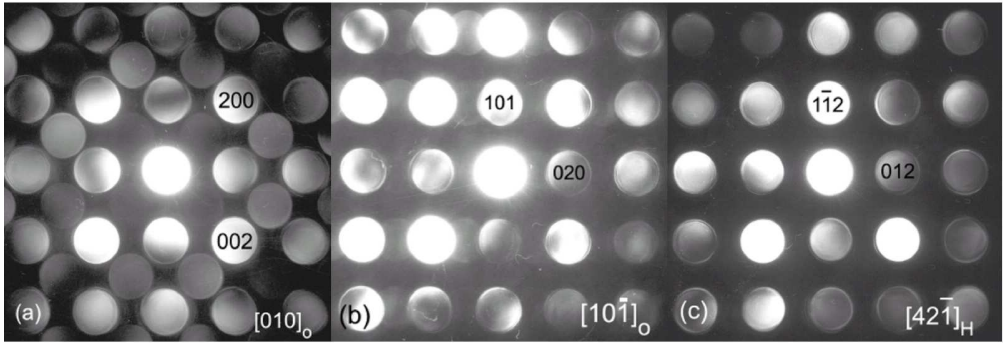


Figure 4  
1130x389mm (72 x 72 DPI)

Peer Review Only

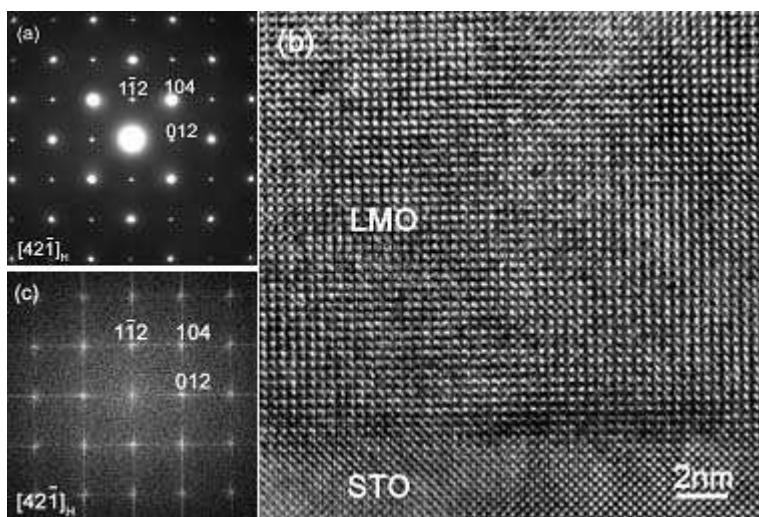


Figure 5  
134x89mm (72 x 72 DPI)